Since January 2020 Elsevier has created a COVID-19 resource centre with free information in English and Mandarin on the novel coronavirus COVID-19. The COVID-19 resource centre is hosted on Elsevier Connect, the company's public news and information website.

Available online at www.sciencedirect.com
ScienceDirect
Virus Research 133 (2008) 88–100
Virus Research
www.elsevier.com/locate/virusres

SARS coronavirus replicase proteins in pathogenesis

Rachel L. Graham [a,c], Jennifer S. Sparks [b,c], Lance D. Eckerle [a,b,c], Amy C. Sims [d], Mark R. Denison [a,b,c,*]

[a] Department of Pediatrics, Vanderbilt University Medical Center, Nashville, TN, United States
[b] Department of Microbiology and Immunology, Vanderbilt University Medical Center, Nashville, TN, United States
[c] The Elizabeth B. Lamb Center for Pediatric Research, Vanderbilt University Medical Center, Nashville, TN, United States
[d] Department of Epidemiology, School of Public Health, University of North Carolina, Chapel Hill, NC, United States

Available online 29 March 2007

Abstract

Much progress has been made in understanding the role of structural and accessory proteins in the pathogenesis of severe acute respiratory syndrome coronavirus (SARS-CoV) infections. The SARS epidemic also brought new attention to the proteins translated from ORF1a and ORF1b of the input genome RNA, also known as the replicase/transcriptase gene. Evidence for change within the ORF1ab coding sequence during the SARS epidemic, as well as evidence from studies with other coronaviruses, indicates that it is likely that the ORF1ab proteins play roles in virus pathogenesis distinct from or in addition to functions directly involved in viral replication. Recent reverse genetic studies have confirmed that proteins of ORF1ab may be involved in cellular signaling and modification of cellular gene expression, as well as virulence by mechanisms yet to be determined. Thus, the evolution of the ORF1ab proteins may be determined as much by issues of host range and virulence as they are by specific requirements for intracellular replication.

Keywords: SARS coronavirus; SARS-CoV; Replication; Pathogenesis; Reverse genetics; Protein processing; Temperature-sensitive mutants; ts mutants

1. Introduction

The coronaviruses express the largest and most complex polyproteins of any RNA viruses. The polyproteins are translated from the genome RNA open reading frames 1a and 1b, and are known as replicase, replicase/transcriptase, or polymerase polyproteins, in recognition of the predicted and demonstrated roles in viral RNA synthesis. However, the appellation of "replicase/transcriptase", while appropriate, is an incomplete description of all probable ORF1ab protein functions. It has been predicted, as well as demonstrated in some cases, that the mature proteins in the polyprotein may serve roles distinct from or in addition to roles in viral RNA synthesis. More specifically, it is becoming clear that proteins or protein domains encoded in ORF1ab may serve specific roles in virulence, virus–cell interactions and/or alterations of virus–host response.

Two events in the history of coronavirus biology have dramatically accelerated the studies and discoveries in protein functions: the SARS epidemic and the development of reverse genetic strategies for the study of coronavirus replication. The rapid identification and sequencing of SARS-CoV isolates led to bioinformatics analyses highlighting both conserved and divergent regions of the replicase genes, particularly in relationship with known group 2 coronaviruses such as mouse hepatitis virus (MHV). In addition, the detailed analysis of animal and human isolates of SARS-CoV during the course of the epidemic revealed evidence of adaptive mutations in the replicase to an extent that matched or exceeded that in the structural proteins.

Concurrently, the rapid establishment of a reverse genetic system for SARS-CoV, as well as the development of reverse genetic systems for other group 2 coronaviruses (Yount et al., 2003, 2002), allowed direct studies of conserved and divergent domains of the replicase in replication. Subsequently, it has become clear that the replicase gene proteins will likely demonstrate multiple functions, many of them novel, in viral pathogenesis. This review will (1) summarize the organization, expression, processing, and putative replication functions of the nonstructural proteins (nsps 1–16) of SARS-CoV; (2) describe studies of ORF1b nsps demonstrating interactions with host cells or host immune response; (3) describe studies of SARS-CoV

* Corresponding author at: 1161 21st Ave S, D6217 MCN, Nashville, TN 37232, United States. Tel.: +1 615 343 9881; fax: +1 615 343 9723.
E-mail address: mark.denison@vanderbilt.edu (M.R. Denison).

0168-1702/$ – see front matter © 2007 Published by Elsevier B.V.
doi:10.1016/j.virusres.2007.02.017

nsps that support functions for the proteins in pathogenesis and adaptation.

1.1. Coronavirus life cycle

Attachment of the virion to the cell surface via a receptor constitutes the first step in the coronavirus life cycle and is perhaps the most important tropism determinant, since coronavirus genomes can replicate in many different cell types when transfected. Receptors vary widely across coronaviruses: for SARS-CoV, human angiotensin converting enzyme 2 (hACE2) can serve as a receptor (Li et al., 2003). Following attachment, the genome enters the cell via a cathepsin L-dependent mechanism (Huang et al., 2006; Simmons et al., 2005). Once inside the cell cytoplasm, the genome serves as an mRNA for the first open reading frame (ORF1), from which the viral replication proteins are translated and processed. These proteins induce and assemble on double-membrane vesicles and become the sites for viral RNA synthesis, and thus comprise the replication complexes. These replication complexes are likely responsible for all viral RNA synthetic activities in the viral life cycle.

Viral RNA synthesis involves two stages: in one stage, input genome RNA is replicated through transcription of a minus-strand template. This is referred to as genome replication. In the other stage, subgenomic mRNAs are transcribed and subsequently used for translation of structural and accessory proteins from downstream ORFs (ORFs 2–9 for SARS-CoV). This stage is referred to as subgenomic RNA transcription and, as it leads to translation of structural proteins, is essential for virion formation and the completion of a productive viral replication cycle (Sawicki and Sawicki, 2005; Sawicki et al., 2007).

All coronaviruses possess four well-characterized structural proteins: S (spike), E (envelope), M (membrane protein), and N (nucleocapsid). These proteins are translated from subgenomic RNAs 2, 4, 5, and 9a, respectively, in SARS-CoV. MHV studies have shown that S, E, and M undergo modification in the Golgi prior to virus assembly (Bost et al., 2000, 2001; Klumperman et al., 1994; Krijnse-Locker et al., 1994). The viral N protein has been shown in MHV to colocalize with viral replicase proteins and at sites of virus assembly at late times post-infection (Bost et al., 2000; Denison et al., 1999; Sims et al., 2000; van der Meer et al., 1999). Viral assembly is precipitated by E and M, which induce a curvature of the budding membrane (Raamsman et al., 2000). Interactions between M, N, and viral RNA lead to S recruitment and RNA packaging into these structures, which form the budding virion (Narayanan et al., 2000; Opstelten et al., 1993, 1995). The viral E protein then aids in the final pinching off of the virion (Fischer et al., 1998). Coronavirus virions are shuttled to the cell surface in large exocytic vesicles, and the virions are released from the cell in a process that does not require cell lysis.

1.2. Coronavirus genome organization and ORF1ab expression and processing

The coronavirus input genome RNA is positive-stranded and functions as an mRNA, from which gene 1 is translated by host–cell ribosomes from two overlapping open reading frames, ORF1a and 1b (Fig. 1). Translation of ORF1a results in a theoretical polyprotein of ∼500 kDa, while translation of ORF1ab results an ∼800 kDa polyprotein (Baranov et al., 2005; Dos Ramos et al., 2004). The ORF 1a and 1ab polyproteins are not detected during infection, since they are most likely processed co- and post-translationally into intermediate and mature proteins by proteinase activities in the nascent polyproteins (Harcourt et al., 2004). The number of proteinases varies by species. All coronaviruses encode a cysteine proteinase in nsp 5 that is referred to as the 3C-like proteinase (3CLpro), or more recently as Mpro (Anand et al., 2003; Tan et al., 2005). The nsp 5 proteinase is responsible for processing the C-terminus of nsp 4 through nsp 16 for all coronaviruses (Anand et al., 2003; Bost et al., 2000; Denison et al., 1998, 1999; Lu et al., 1998; Tan et al., 2005). In contrast, nsps 1–3 are cleaved by either one or two papain-like proteinase activities (PLP) within nsp 3 (Anand et al., 2003; Bonilla et al., 1995, 1997; Dong and Baker, 1994; Harcourt et al., 2004; Kanjanahaluethai and Baker, 2001; Snijder et al., 2003; Tan et al., 2005; Teng et al., 1999; Ziebuhr et al., 2000). Group 1 (HCoV-229E) and group 2a (MHV) coronaviruses each encode PLP1 and PLP2, while group 2b (SARS-CoV) and group 3 (Avian infectious bronchitis virus—IBV) coronaviruses each encode only one PLP in the position of PLP2. IBV possesses an inactive remnant of PLP1, while SARS-CoV PLP1 appears to have been completely lost (Snijder et al., 2003) (Fig. 2). Regardless of the number of PLPs present, nsps 1–3 are processed by papain-like proteinase(s) for all coronaviruses. These distinct processing networks may serve to regulate the liberation of intermediate and mature protein species that perform conserved functions across coronavirus groups.

1.3. Evolution and adaptation

Prior to the SARS epidemic, studies of coronavirus evolution were limited to established laboratory virus strains, and focused exposure to chemical mutagens and subsequent analysis of adapted strains. The most elegant work came from studies of gradual adaptation of MHV to Syrian baby hamster kidney (BHK) cells. The resulting passaged virus grew efficiently in murine, hamster, human, and primate cells, clearly demonstrating the ability of coronaviruses to cross species barriers (Baric et al., 1997). This report was remarkably prescient, coming less than 10 years before the natural experiment of SARS-CoV transmission from animals into humans. The SARS epidemic created a unique opportunity to study the changes in an animal virus as it encountered a previously unexposed human population, both geographically and temporally. A study of 63 isolates of SARS-CoV, including animal and human strains was performed by the Chinese SARS consortium to determine rates of mutation along the course of the epidemic (Chinese, 2004). Complete sequencing of the isolates allowed detailed direct and statistical analysis of adaptation in SARS-CoV, and it led to conclusions about the most variable regions of the genome during the course of the epidemic. As expected, the S coding region demonstrated the most mutations resulting in non-synonymous amino acid

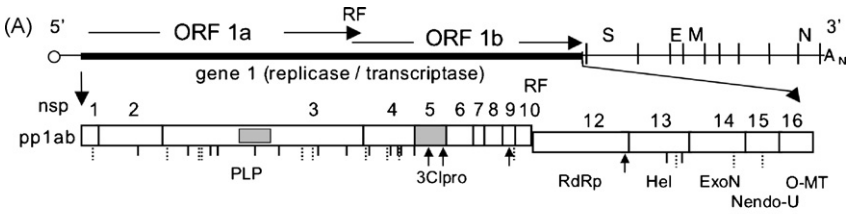

(B)

Replicase ORF1ab amino acid substitutions	
nsp1	**C82G**
nsp2	A549S
nsp3	**W832L** A1021V T1121I **P1136L** A1233V R1319K I1663L A1900V **F2116L Y2222C** L2269S A2552V
nsp4	**W2746C Y2770L I2944T S2949F** A2971V A3047V **F3062V** A3072V A3197V
nsp5 (3CLpro)	MA-H3374A MA-E3510A
nsp9	**G4154E** MA-T4184A
nsp12 (RdRp)	MA-A5292V
nsp13 (Hel)	S5623L **P5720S** E5767D
nsp14 (Exo N)	**T6274I**
nsp15 (Nendo U)	**P6540L**

Fig. 1. SARS-CoV genome organization, ORF1ab protein expression and amino acid substitutions. (A) Genome and ORF1ab organization. The SARS-CoV genome is a positive-strand RNA molecule ∼29 kb in length. The organization of ORF1a and 1b is shown, with the position of the −1 ribosomal frameshift indicated (RF). The remaining genes are indicated by vertical lines, and notation for genes encoding spike (S), envelope (E), membrane (M) and nucleocapid (N). The polyprotein resulting from translation of ORF1ab is shown (pp1a), with vertical lines and nonstructural (nsp) numbers 1–16. Nsp 11 is a theoretical 13aa peptide (not shown). The papain-like proteinase (PLP) of nsp 3 and 3C-like proteinase (3CLpro) of nsp 5 are grey boxes. The location of the PLP1 enzyme present in MHV but not SCoV is indicated by grey box with hatched border. Activities are indicated for nsp 12 (RNA-dependent RNA polymerase—RdRp), nsp 13 (helicase—Hel), nsp 14 (3′–5′ exoribonuclease—ExoN), nsp 15 (endoribonuclease—NendoU), and nsp 16 (2′-*O*-methyltransferase—*O*-MT). Solid and dashed lines below the ORF1ab proteins indicate location of conservative and non-conservative nonsynonymous adaptive substitutions, respectively. Arrows indicate location of mutations in mouse adapted SARS-CoV. (B) Location of evolutionary adaptive and mouse adaptive mutations. Nsp numbers are indicated, with table showing adaptive mutations, non-conservative changes (bold) and mouse adaptive mutations (MA) by residue number and substitution.

substitutions, at a rate indicating significant positive selective pressure, and in a manner suggesting early rapid change and late purifying adaptive changes (Chinese, 2004). Surprisingly, however, the ORF1a polyprotein showed a rate of nonsynonymous substitutions similar to that in the S gene, also tracking with early rapid change and late purifying mutations (Fig. 1). The ORF1b polyprotein, in contrast, had little evidence of rapid change or positive selective pressure.

In addition, the data in that report suggests that the changes in the replicase may be even more significant. Specifically, in the S coding region (1255aa) there were 22 nonsynonymous variations (NSV), of which 11 were nonconservative changes. In ORF1ab,

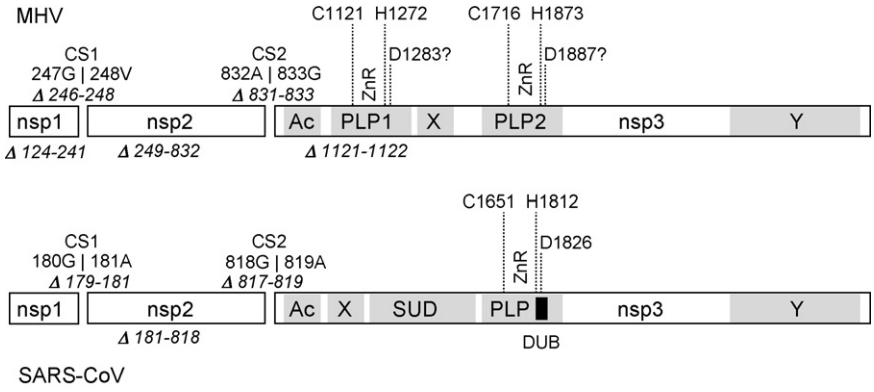

Fig. 2. Organization of and viable mutants generated within coronavirus nsps 1–3. The organization and predicted and confirmed domains of MHV and SARS-CoV nsps 1–3 are shown. Gray boxes indicate discrete domains within nsp 3. The nsps 1–2 and 2–3 cleavage sites (CS1 and CS2, respectively) are delineated by amino acid number. Catalytic Cys, His, and Asp residues for each PLP are indicated by amino acid number. Deletion of cleavage sites and portions of or whole proteins, and the inactivation of the MHV PLP1 catalytic site are indicated by delta (Δ) signs, and the deleted amino acid residues are indicated. Domains within nsp 3 are as follows—Ac: acidic domain; PLP1: papain-like proteinase 1; X: X domain (ADP ribose 1″-phosphatase activity); PLP2: papain-like proteinase 2 (SARS PLP is orthologous to MHV PLP2); ZnR: zinc ribbon domains within PLPs; DUB: Core motif for deubiquitinating activity; Y: Y domain.

there were 29 NSV, of which 14 were nonconservative. When ORF1a (4369aa) is considered alone, there were 24 NSV with 11 nonconservative substitutions. Even more impressive, nsp 3 (1921aa) had 12 NSV, five of which were nonconservative, and the smaller nsp 4 (500aa) had nine NSV of which four were nonconservative. This was in contrast to six NSV (four nonconservative) in all of ORF1b (2703aa). These results support the conclusion that adaptations during the SARS epidemic, with transmission from animals and among humans, was associated with substantial changes in ORF1a, notably focused in nsps 3 and 4. These proteins are discussed in subsequent sections, but the overall analysis suggests they may be important for survival and adaptation in the host and thus may serve functions that are distinct from replication.

The adaptation of SARS-CoV observed in the Chinese Consortium studies was based on introduction into humans, presumably from animals that functioned as replication intermediates, transmitting a SARS-CoV precursor virus from a different stable animal reservoir (Chinese, 2004). The rates and loci of changes are strong evidence for positive selective pressure and adaptation for virulence and maintenance in human populations. However, the analysis was not a prospective study of the capacity of SARS-CoV to adapt in a new species. Such a study was performed by adaptation of SARS-CoV to virulence in mice. Mice are known to support the replication of human isolates of SARS-CoV, but replication is limited and without pathogenic correlates or mortality in young mice (Yount et al., 2005). When the SARS-CoV Urbani strain was passaged 15 times in young mice, virus obtained at passage 15 (MA-15) demonstrated rapid and reproducible lethality in the same mouse strain (Roberts et al., 2007). Sequencing of the entire genome of the MA-15 virus identified six mutations resulting in nonsynonymous substitutions. Surprisingly, of the six mutations, four were in ORF1ab, with two in nsp 5, one in nsp 9 and one in nsp 12 (Fig. 1). The other two mutations were identified in structural ORFs: one in ORF 2 (S), and one in ORF 5 (M). The genetic recapitulation of the four-replicase mutations alone increased the virulence of SARS-CoV in mice, and all six-substitution mutations restored the full virulence of the MA15 virus. This is strong evidence that virulence-conferring mutations in ORF1ab are positively selected during trans-species transmission of SARS-CoV and SARS-like coronaviruses. Interestingly, it suggests that even conservative nonsynonymous changes (e.g., Ala to Val) may be important for virulence changes or replication in a new host.

2. Materials and methods

2.1. Viruses and cells

A recombinant form of severe acute respiratory syndrome coronavirus Urbani strain (SARS-Urbani, or SARS-CoV in this report) was used as the wildtype control in all SARS-CoV experiments. SARS-CoV Urbani reference sequence AY278741 was used for cloning studies. African green monkey kidney (Vero-E6) cells were grown in MEM that contained 10% FBS for SARS-CoV experiments.

2.2. Antibodies

The rabbit polyclonal antibodies described in the experiments in this report have been previously described. They include α-nsp 1 (VU232), α-nsp 2 (VU239), and α-nsp 8 (VUGP14) (Graham et al., 2005; Graham et al., 2006; Prentice et al., 2004b).

2.3. Construction of mutant SARS-CoV viruses

Deletions and amino acid substitutions at and near SARS-CoV CS1 were achieved using site-directed mutagenesis of SARS-CoV fragment A as before (Graham et al., 2005; Graham et al., 2006). Primers used in mutagenesis are described in Table 1. For all primer sets, PCR was performed from wildtype SARS-CoV fragment A, generating A–B and C–D amplicons. The resulting amplicons were then digested with *Bbs* I, ligated to form ABCD products, and inserted into the fragment A background using native *Nci* I and *Nco* I restriction sites. Full-length cDNAs were then assembled and mutant viruses recovered as detailed in Graham et al. (2005), Graham et al. (2006) and Yount et al. (2003).

2.4. Protein immunoblots

SARS-CoV-infected cells were lysed in inactivation buffer containing 20 mM Tris–HCl pH 7.6, 150 mM NaCl, 0.5% DOC, 1% Nonidet P-40, and 0.1% SDS, and tested to confirm inactivation (Darnell et al., 2004). Following centrifugation at 16,000 × *g* for 2 min to pellet nuclei, supernatants were treated with 1 volume of 10 mM EDTA/0.9% SDS. Lysates were then heated at twice at 90 °C for 30 min prior to use. Immunoblots to detect SARS-CoV proteins were then performed as described in Prentice et al. (2004b). Images were processed using Adobe Photoshop CS.

Table 1
Primers used in mutagenesis of SARS-CoV CS1

Primer name	Sequence	Sense	Purpose
SCS1 A	5′-CCGGGTGTGACCGAAAGGTAAGATGGAGAGCCT-3′	+	Common left primer (A + B)
SCS1 D	5′-CCATGGCGTCGACAAGACGTAATGACTGTTCAGA-3′	−	Common right primer (C + D)
A1 B	5′-GAAGACGCCAATGTCACTCGCTATGTCGACAAC-3′	+	Mutagenesis of CS1 P2–P1′
A1 C	5′-GAAGACGGATTGAGCTCACGAGTGAGTTCACG-3′	−	Mutagenesis of CS1 P2–P1′
A4 B	5′-GAAGACGGGAAGTACTGCTGCCGTGACCATGA-3′	+	Mutagenesis of MHV-like RGV
A4 C	5′-GAAGACGGCTTCGACTCGATGTAATCAAGTTGTT-3′	−	Mutagenesis of MHV-like RGV
A2 B	5′-GAAGACCCGTGTCACTCGCTATGTCGACAACAAT-3′	+	Mutagenesis of CS1 P1′
A2 C	5′-GAAGACCCACACCACCTCCATTGAGCTCACGAG-3′	−	Mutagenesis of CS1 P1′

2.5. Indirect immunofluorescence detection of viral proteins

Vero-E6 cells were grown to 60% confluency on 12 mm glass coverslips and infected with wildtype or mutant viruses. At 12 h p.i. and 20 h p.i., medium was aspirated from cells, and cells were fixed and permeablized in −20 °C methanol overnight. Coverslips were transferred to clean 24-well plates containing fresh methanol prior to removal from BSL-3 conditions. Cells were then rehydrated in PBS for 20 min, then blocked in PBS containing 5% bovine serum albumin (BSA). The following steps were performed in immunofluorescence assay (IFA) wash solution (PBS containing 1% BSA and 0.05% Nonidet P-40) at room temperature. Blocking solution was aspirated, and cells were incubated with primary antibodies at 1:200 dilution for 1 h. Cells were then washed in IFA wash solution three times for 10 min per wash. Cells were then incubated in secondary antibodies (Goat α-rabbit-Alexa 488, 1:1000, and Goat α-guinea pig-Alexa 546, 1:1000, Molecular Probes) for 45 min. Cells were washed again three times for 10 min per wash, followed by a final wash in PBS, and then rinsed in distilled water. Coverslips were mounted with Aquapolymount (Polysciences) and visualized by confocal immunofluorescence microscopy on a Zeiss LSM 510 laser scanning confocal microscope at 488 and 543 nm with a 40× oil immersion lens. Images were processed and assembled using Adobe Photoshop CS2 (9.0.2).

3. Results and discussion

3.1. Nonstructural proteins: adaptation and virulence

The above studies demonstrated by comparative analysis and selection in an animal host the importance of ORF1ab proteins in host adaptation and virulence. Our work and that of others has focused on defining protein domains within ORF1ab that are involved in replication, innate immune response and virulence. A methodical approach has been taken towards determining the requirement and functions of MHV nsps 1–16 in replication. To that end, numerous amino acid residues, proteins, and protein domains have been identified that are dispensable for replication but whose modification leads to attenuation in animals. These observations have been applied by identifying the orthologous protein domains or amino acid residues of SARS-CoV and using reverse genetic approaches to introduce the same modifications in SARS-CoV. Together, the results demonstrate that proteins or protein domains of ORF1ab are critical for efficient replication and virulence in SARS-CoV. In addition, it has become clear through these studies that nsp order, expression level, and proteolytic processing may constitute distinct virulence alleles.

3.2. Nsps 1–3

The first approximately 2700 aa of the ORF1ab polyprotein comprise the nsps 1–3 proteins (Fig. 2). This region of ORF1ab is the most variable among coronaviruses. As a group 2b coronavirus, SARS-CoV and the related SARS-like animal viruses have similar organization and protein sizes as other group 2 coronaviruses, with the distinction that nsps 1–3 are processed by a single PLP. Alignment of ORF1ab protein sequences of SARS-CoV with MHV or other group 2a coronaviruses reveals significant identity and similarity in nsps 4–16, but very limited identity or similarity of nsps 1–3. When the variability between nsp 3 isolates of the SARS epidemic are compared, the results suggest that nsps 1–3 perform cell- and host-specific roles in replication and/or virulence. Additionally, they have demonstrated high capacity for adaptation to new environments and selective pressures. As a result, it is likely that these proteins play dual roles in replication and pathogenesis that may vary widely between virus groups.

3.2.1. Nsp 1

Two recent studies of SARS-CoV nsp 1 suggest that this protein of ORF1ab may play specific roles in the interaction of the virus with the innate immune response. Kamitami et al. observed that SARS-CoV replication in human 293 cells suppresses IFN-β mRNA accumulation (Kamitani et al., 2006). Plasmid-based overexpression of nsp 1 resulted in the inhibition of host gene expression by promoting degradation of host mRNA, and that IFN-β mRNA accumulation was decreased without alteration of IRF-3 phosphorylation, dimerization, or translocation. Further analysis showed that SARS-CoV nsp 1 suppressed Sendai virus-induced IFN-β mRNA accumulation, and suppressed reporter mRNA accumulation in cells. Degradation of preexisting mRNAs resulted in an overall inhibition of cellular protein synthesis. The authors conclude that the degradation of host mRNA would inhibit immune response genes such as IFN-β, and thus, that nsp 1 is likely a virulence factor.

Overexpression of nsp 1 in the lung epithelial cell line A549 increases the production of CCL5, CXCL10 and CCL3 cytokines 30–200-fold compared with mock-transfected cells or cells expressing nsp 5 (Law et al., 2006). Similar results were detected with CCL5 and CXCL10 in HepG2 cells, suggesting that this was not a cell line-specific induction. NFκ-B expression increased 10–14 h post-nsp 1 transfection, suggesting that cytokine induction occurred via an NFκ-B-dependent pathway. In support of this hypothesis, expression of CCL5, CCL3 and CXCL10 was reduced up to 60% in nsp 1-expressing cells in the presence of the IKK-β inhibitor, sodium salicylate. In contrast, the cytokine induction was not detected upon expression of nsp 1 of the group 2a coronaviruses MHV and OC43, nor with that of the group 1 coronavirus HCoV-229E. The authors conclude that expression of SARS-CoV nsp 1 plays a role unique to the group 2-like coronaviruses in the regulation of chemokine expression.

These two recent reports suggest that SARS-CoV nsp 1 may serve multiple roles in pathogenesis. Whether the protein is also required for virus replication remains to be determined. Mutagenesis and deletion studies of MHV nsp 1 indicate that the protein can tolerate substitution of clustered charged residues, as well as deletion of the carboxy-terminal half of the protein, and still support recovery of viable virus with modest replication defects (Fig. 2) (Brockway and Denison, 2005). However, the lack of effect of MHV nsp 1 in the chemokine study, as well as the limited amino acid identity (<20%) between MHV and SARS-CoV nsp 1 proteins, suggest that there may

be more differences than similarities in these proteins. The studies also raise the question of how nsp 1 can simultaneously induce host mRNA degradation and specific gene expression. Confirmation of these results in 293, A549, and HepG2 cells, as well as other naturally permissive and ACE 2-expressing cell lines, will be crucial to reconcile these results. Finally, it will be critical to test these in vitro results during virus infection in cells, specifically with genetically defined mutants of nsp 1, to determine if mutations in nsp 1 alter the replication or pathogenesis of SARS-CoV in defined animal models.

3.2.2. Nsps 2 and 3

The functions of nsp 2 are entirely unknown, while nsp 3 has multiple conserved domains, including PLP activity, as well as putative functions in replication complex formation and viral RNA synthesis and processing (Putics et al., 2005; Snijder et al., 2003). However, recent studies with MHV and HCoV-229E suggest that all or portions of these proteins may have functions in pathogenesis.

The nsps 2 and 3 proteins of MHV have been extensively studied using reverse genetic mutation, deletion and modification of cleavage sites and viral proteinases. Nsps 2 and 3 of MHV and SARS CoV are detected as mature processed proteins but also as nsps 2 and 3 intermediate precursors (Denison et al., 1992; Graham et al., 2005; Harcourt et al., 2004; Schiller et al., 1998), suggesting that the nsps 2 and 3 precursor may be important in replication, possibly serving distinct roles or regulating availability of mature nsps 2 and 3 proteins. The requirement for processing of nsps 1–3 has been tested by engineered deletion of the cleavage sites between nsps 1 and 2 and between nsps 2 and 3 (Fig. 2) (Denison et al., 2004; Graham and Denison, 2006). In MHV, deletion of the nsp 1 | nsp 2 cleavage site resulted in recovery of infectious virus with less than a $1 - \log_{10}$ reduction in peak virus titer in culture (Denison et al., 2004). Deletion of the nsp 2 | nsp 3 cleavage site allowed recovery of virus that could not process mature nsps 2 and 3 (Graham and Denison, 2006). Recovered viruses grew to wildtype peak titer, but demonstrated delays in the initial increase in virus titer compared to wildtype virus and other mutants that did not abolish cleavage of nsps 2 from 3. Nsp 1 | nsp 2 and nsp 2 | nsp 3 cleavage site deletions have been engineered into SARS-CoV and are being tested for their effects on replication and pathogenesis in mice.

These results suggest that nsp 2 may regulate functions of nsps 1 and 3. Therefore, the entire coding sequence of nsp 2 was deleted in both SARS-CoV and MHV, resulting in an in-frame nsp 1 | nsp 3 junction containing a "new" chimeric nsp 1 | nsp 3 cleavage site. Surprisingly, the nsp 2 deletion mutants of SARS-CoV and MHV were both viable, and were both able to process the chimeric nsp 1 | nsp 3 cleavage site. The resulting mutant viruses had decreased but not delayed growth. Together, these results indicate that the nsp 1 | nsp 2 cleavage site, the nsp 2 | nsp 3 cleavage site, and in fact the entire nsp 2 protein, are dispensable for replication in culture (Fig. 2). Thus, there is no absolute replication requirement for the mature nsps 1, 2, or 3 proteins of MHV or SARS-CoV. More intriguing is the complete dispensability of nsp 2. The ability to test a complete nsp 2 deletion with retained nsps 1 and 3 maturation will allow the study of the role of nsp 2 in replication and pathogenesis in animal models.

As with nsp 2, in vitro and reverse genetic studies of specific domains of nsp 3 from MHV and HCoV-229E have provided important insights into possible roles in replication and pathogenesis. The Appr-1″-p domain of nsp 3 is proposed to have functions in viral RNA synthesis (Snijder et al., 2003). Putics et al showed that the nsp 3 Appr-1″-p subdomain of both SARS-CoV and HCoV-229E, when expressed alone in vitro, possess Appr-1″-p activity and that the activity is abolished by substitutions at predicted catalytic residues (Putics et al., 2005). However, when the inactivating mutation was engineered in recombinant HCoV-229E, no change was seen in virus growth or RNA synthesis, demonstrating that the Appr-1″-p activity is not essential for replication in culture, and raising questions about its role in the infected host.

The PLP activities of nsp 3 may also serve roles in replication and pathogenesis that could involve unique mechanisms or interactions with the host cell. SARS-CoV contains only a single PLP, orthologous to MHV PLP2. The SARS PLP has been purified and shown to cleave between nsp 1 | nsp 2, nsp 2 | nsp 3, and nsp 3 | nsp 4 and to recognize and cleave following a P4-L(N/K)GG-P1 sequence, with no clear requirement in the P1′ position. The L(X)GG motif was noted to be similar to the recognition site of cellular deubiquitinating enzymes. Two groups subsequently demonstrated that expressed and purified SARS PLP possesses deubiquitinating activity (Barretto et al., 2005; Lindner et al., 2005). The structure of the SARS-CoV core catalytic PLP (aa1541–1855) was subsequently reported, demonstrating the structural correlates of the biochemical results, and further confirming the recognition of the core P4-LXGG-P1 (Ratia et al., 2006). The mechanism and role of deubiquitinating activity of SARS PLP in replication remains to be determined, but the efficiency of deubiquitinating activity of SARS-CoV PLP on artificial substrates suggests that it may be playing a role in modification of host cell proteins, possibly in addition to recognition of the LXGG motif in viral polyproteins. Finally, it has been shown that the SARS PLP can recognize and cleave peptides containing the PLP cleavages sites of the group 2a viruses MHV and BCoV, but not the group 1 HCoV-229E, supporting the phylogenetic grouping of SARS-CoV as a group 2b coronavirus and suggesting that studies of MHV may be most relevant to the further understanding of SARS-CoV processing and PLP activities (Han et al., 2005).

In that regard, it has recently been demonstrated that MHV, which contains PLP1 and PLP2 proteinase activities in nsp 3, can be engineered with an inactivation of PLP1, resulting in abolished cleavage at nsp 1 | nsp 2 and nsp 2 | nsp 3 (Fig. 2) (Graham and Denison, 2006) and an uncleaved nsps 1–3 precursor. These PLP1 mutants were highly impaired on recovery, but adapted over passage to regain near wildtype growth in culture without reversion of PLP1 inactivating mutations and without cleavage of nsps 1 from 2 and 3. Multiple putative adaptive mutations have been identified, including mutations in nsp 3 in the Appr-1″-p and PLP2 domains, and these, both alone and together, have been confirmed to partially compensate growth (Graham and Denison, unpublished results). Interestingly, monitoring the

introduction of mutations in the complete genome over 27 virus passages in culture identified new mutations in ORF1a, ORF1b, S, and N. In addition, changes in the leader and transcriptional regulatory sequences correlated with increased growth fitness. These observations suggest that the ORF1ab proteins, notably nsp 3, may interact with multiple structural and nonstructural proteins, as well as with regulatory sequences in viral RNA. Thus, it is likely that additional functions in replication and pathogenesis will be defined for nsp 3.

3.2.3. Processing at the nsp 1 | nsp 2 cleavage site (CS1)

While SARS-CoV is similar to group 2 coronaviruses such as MHV in many ways, it differs in the processing of nsps 1 and 2. As has been discussed, SARS-CoV mediates processing of the nsp 1 | nsp 2 and nsp 2 | nsp 3 cleavage sites (CS1 and CS2, respectively) with its single PLP, which is a PLP2 ortholog, rather than with a PLP1-like activity as is observed in MHV infection (Harcourt et al., 2004; Snijder et al., 2003). However, SARS-CoV encodes an RG | V amino acid sequence (aa 226–228), similar to that encoded at the MHV CS1, which is C-terminal from the GG | A amino acid tripeptide (aa 179–181) that serves as the SARS-CoV CS1. To determine if the RG | V sequence was recognized by the SARS-CoV PLP in the context of infection, three-amino acid deletions of $_{226}$RG | V$_{228}$ and $_{179}$GG | A$_{181}$ were engineered into the SARS-CoV genome (mutants A4 and A1, respectively) using reverse genetics (Fig. 3A). Additionally, a single-amino acid substitution at the CS1 P1′ position was generated (Ala181Gly, mutant A2) which was predicted to allow processing at CS1 to occur. All three mutants resulted in the recovery of infectious virus. Upon examination of the nsps 1, 2, and 8 proteins in infected cells by immunoblot, we confirmed that the $_{179}$GG | A$_{181}$ deletion resulted in the loss of processing at CS1, as evidenced by the lack of detection of mature 20 kDa nsp 1 and 70 kDa nsp 2 products (Fig. 3B). Immunoblotting with both nsps 1 and 2 antibodies resulted in the detection of a protein with a mobility of approximately 90 kDa, which corresponds to the predicted size of an uncleaved nsp 1–2 precursor. Infection with the A2 and A4 mutants did not disrupt processing at CS1, and there was no evidence of alternative processing at the $_{226}$RG | V$_{228}$ site in the A4 mutant. Interestingly, in the A1 mutant infection, additional proteins normally detected in infected cells with nsp 2 antiserum with approximate mobilities of 42 and 100 kDa also evidenced shifts that corresponded to increases of 10–20 kDa in size. These products, which were not detected in wildtype or other mutant infections with nsp 1 antiserum, were detected in infections with the A1 mutant with nsp 1 antiserum, suggesting that these bands represent nsp 2-containing intermediates or further processing products in the wildtype infection and that these products are similarly processed in the A1 infection in spite of the lack of processing at CS1. This processing strategy of nsp 2 is distinct from that observed with MHV-A59 infection, but is reminiscent of that observed with MHV-JHM infection, in which a 72 kDa nsp 2-containing species is further processed into a "mature" 65 kDa nsp 2 (Gao et al., 1996; Schiller et al., 1998). The processing determinants of these possible alternative forms of nsp 2 in SARS-CoV are not currently known.

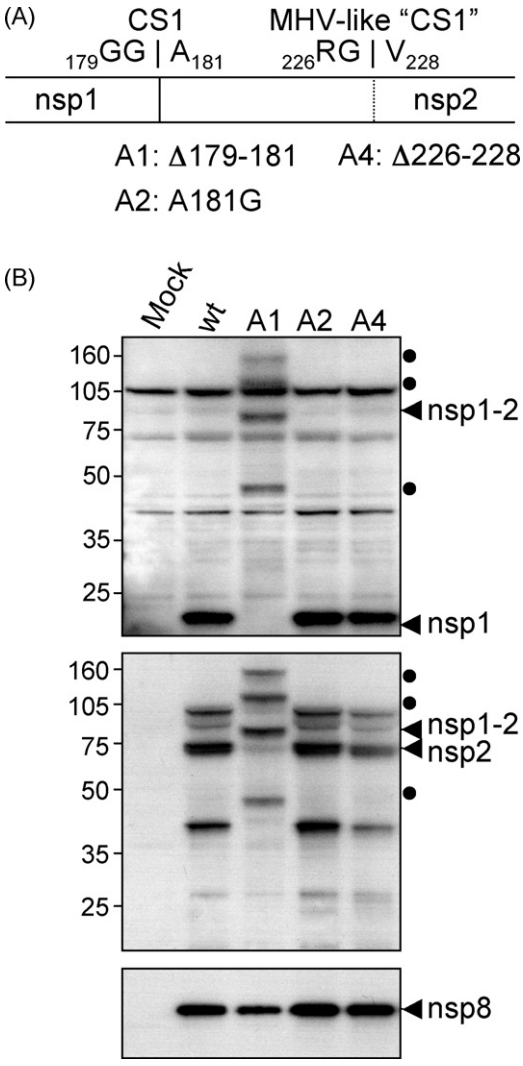

Fig. 3. Mutation of SARS-CoV CS1 and identification of nsps 1 and 2 precursor. (A) The schematic shows locations of experimentally identified CS1 and MHV-like RG | V recognition sequence. Mutants generated are identified beneath the schematic. Numbering refers to amino acid sequence from the beginning of ORF1a. (B) Immunoblot of mock- and SARS-CoV-infected lysates. Mutant designations are as in A. Vero cells were infected with indicated viruses, harvested at 12 h p.i., and resolved by SDS-PAGE. Antibodies used are against nsp 1 (top), nsp 2 (middle), and nsp 8 (bottom). Molecular weights are indicated to the left of the images. Protein bands are indicated with arrows to the right of images. Putative precursors and maturation products are indicated with circles.

3.2.4. Replication complex localization of nsps 1 and 2

It has been shown that, for MHV, nsps 1 and 2 localize to replication complexes (Bost et al., 2000; Brockway et al., 2004; Sims et al., 2000). While MHV nsp 2 localization to replication complexes is stable throughout the course of infection, MHV nsp 1 localization is less stable. The interaction of MHV nsp 1 with membrane populations has been shown to be largely peripheral in biochemical studies, and at late times post-infection, nsp 1 exhibits characteristics similar to nsp 13 (hel) and nucleocapsid (N) proteins, which have been shown to translocate to sites of virion assembly (Brockway et al., 2004; Sims et al., 2000). To determine if SARS-CoV nsps 1 and 2 behave similarly to MHV nsps 1 and 2, Vero cells were infected with wildtype, A1,

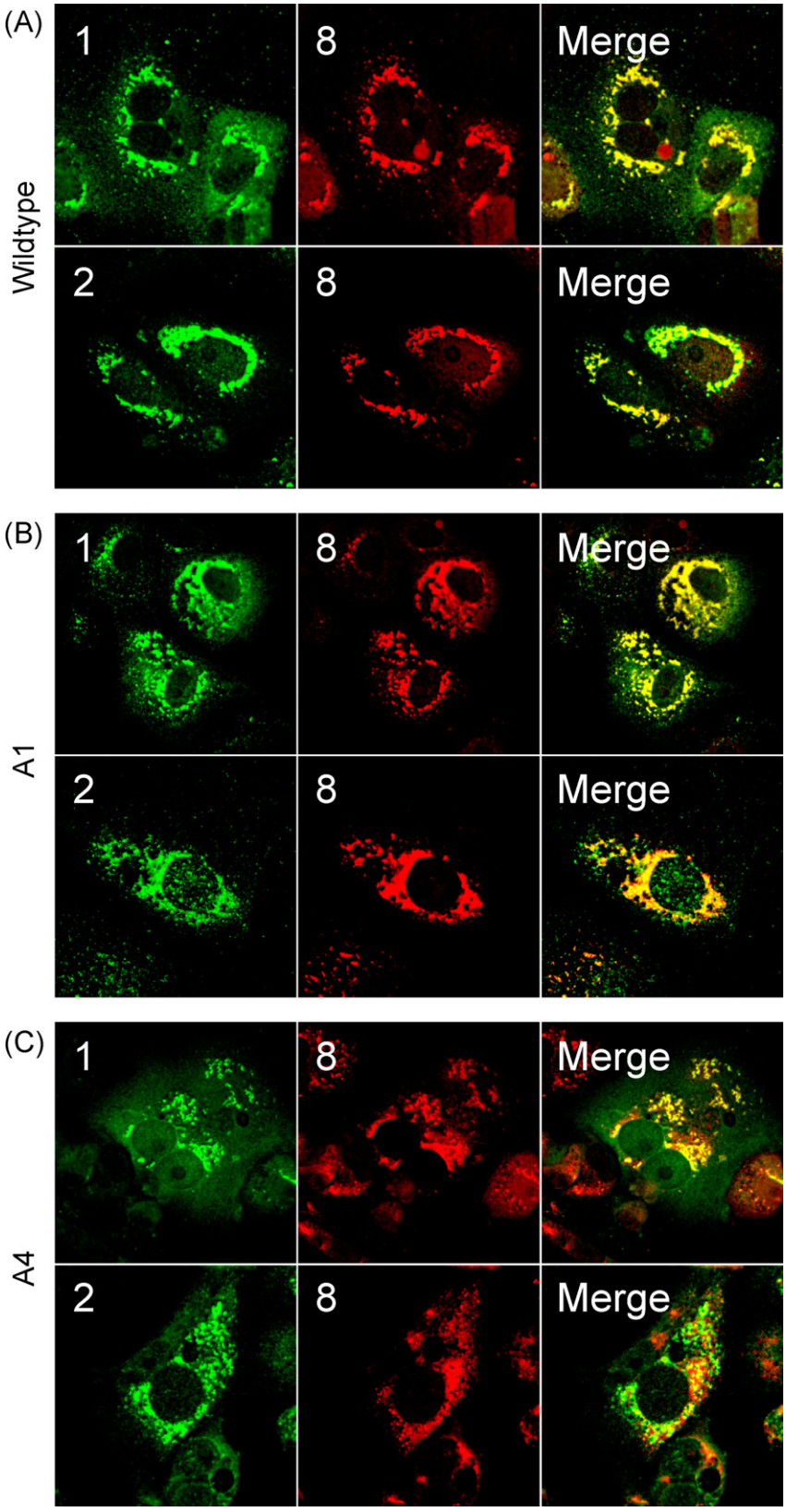

Fig. 4. Immunofluorescence of SARS-CoV-infected cells. Vero cells on glass coverslips were infected with wildtype (wt, A), A1 (B), or A4 (C) viruses. Mutant designations are as outlined in Fig. 3. Cells were fixed and permeablized with methanol at 12 h p.i. Fixed coverslips were then stained for nsps 1 or 2 along with nsp 8 as a marker for replication complexes. Images were obtained using a Zeiss LSM 510 confocal microscope and were processed using Adobe Photoshop CS2 (9.0.2).

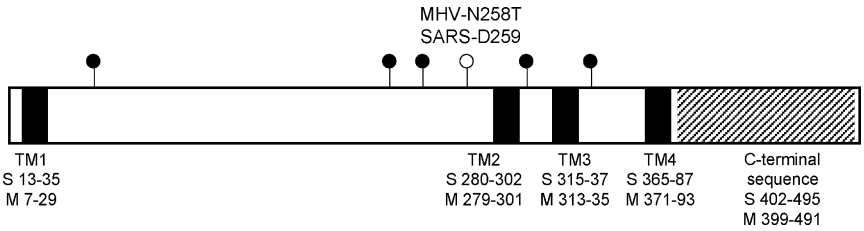

Fig. 5. Schematic of MHV and SARS-CoV nsp 4 motifs, deletions and mutations. The schematic shows the aa organization of MHV (496aa) and SARS-CoV (500aa) nsp 4. Black boxes show the location and sequences of predicted transmembrane domains 1–4 (TM-1–4) with the predicted aa boundaries for MHV (M) and SARS-CoV (S). TM4 has been deleted in viable MHV mutants. The hatched box shows the region of the MHV nsp 4 carboxy terminus that has been deleted in a viable mutant, and the corresponding SARS-CoV aa sequence, Note that the nsps 4 and 5 cleavage site was not deleted. Black circles show the location of clustered charge-to-alanine mutants viable in MHV and conserved in SARS-CoV. The white circle shows the location of the published MHV Alb ts6 mutation (N258T) and the corresponding SARS-CoV D259 residue.

or A4 mutants, cells were fixed and permeablized, and nsps 1 and 2 proteins were visualized by indirect immunofluorescence assay (Fig. 4). At 12 h post-infection (p.i.), wildtype nsps 1 and 2 both displayed bright, punctate perinuclear localization, similar to that observed in MHV infection (Fig. 4A). Both proteins colocalized with nsp 8, another replicase protein and a marker for replication complexes. Similar patterns of localization were observed at 20 h p.i., which was expected for nsp 2, but which was distinct from that shown for nsp 1 in MHV infection (data not shown). Infection with the A1 mutant resulted in a similar pattern of localization for both nsps 1 and 2 (Fig. 4B). Surprisingly, the A4 mutant, which displayed nsp 1 localization patterns similar to what was seen in wildtype and A1 infection, evidenced an altered localization of nsp 2 in relation to the replication complex marker, nsp 8 (Fig. 4C). While nsp 2 localization was still punctate, its pattern did not closely match that observed for nsp 8 (indicated by the reduction in the proportionate number of yellow pixels in the merged image). This data suggests that the deletion of the $_{226}$RGV$_{228}$ in the A4 mutant may disrupt a domain of nsp 2 required for proper replication complex interaction, though the formation of the replication complexes is apparently not hindered, as evidenced by the localization of nsps 1 and 8. We have previously shown for MHV that nsp 2 is not required for replication complex formation (Graham et al., 2005), and while it is not surprising that such is the case for SARS-CoV, it is intriguing that nsp 2 localization to punctate structures in the cytoplasm appears only altered rather than completely abolished.

3.3. Nsp 4

The nsp 4 protein is also referred to as MP1 (membrane protein 1) for its multiple highly hydrophobic stretches of amino acids predicted to span intracellular membranes (Fig. 5) (Bonilla et al., 1994). Together, nsps 3, 4, and 6 are predicted to function to nucleate and anchor viral replication complexes on double-membrane vesicles in the cytoplasm (Gosert et al., 2002; Prentice et al., 2004a; van der Meer et al., 1999). Nsp 4 is the N-terminal-most ORF1ab protein that shares greater than 50% identity and similarity with other coronavirus groups, suggesting that nsp 4 protein function is important or essential for viral replication. Prior to the establishment of a coronavirus reverse genetic system, analysis of nsp 4 began at the level of identification of cleavage sites and proteases responsible for liberating the protein from the polyprotein. It was discovered that SARS-CoV nsp 4 is cleaved first at its amino terminus by the PLP (PLP2 for MHV) and at its carboxy terminus by 3CLPro (Harcourt et al., 2004; Kanjanahaluethai et al., 2003; Prentice et al., 2004b). After nsp 4 has been cleaved from the ORF1a polyprotein at its carboxy terminus, it can be detected as an intermediate precursor product that includes nsps 4–10 and has an approximate mass of 150 kDa (Kanjanahaluethai et al., 2003). It is predicted that intermediate products may play important roles during either replication or pathogenesis of coronaviruses. The second cleavage event of nsp 4 is mediated by nsp 5, generating for MHV a protein with a predicted mass of 56 kDa but an apparent mass of 44 kDa and for SARS-CoV a protein with a predicted mass of 55 kDa but an apparent mass of 35 kDa (Kanjanahaluethai et al., 2003; Lu et al., 1996; Prentice et al., 2004b).

As described above, SARS-CoV nsp 4 showed evidence for substantial adaptation over the course of the epidemic, with the rate of NSV and nonconservative substitutions equivalent to that in S (Chinese, 2004). Based on these studies, deletions and alanine substitution of clustered charged residues were engineered in MHV nsp 4, targeting residues that are identical in SARS-CoV nsp 4 (Fig. 5). Using this approach, nsp 4 mutant viruses have been recovered that have multiple plaque and growth phenotypes, ranging from small plaque size and decreased growth, to wild type plaque size and growth (Sparks et al., unpublished results). Most surprising, nsp 4 tolerated deletion of the carboxy-terminal 100 aa, or 20% of the coding sequence, and the mutant virus with this deletion had no detectable growth defect compared to wild type virus. The nsp 4 carboxy-terminal deletion has been cloned for introduction into the SARS-CoV genome. If infectious virus is recovered, this will be a strong candidate for evaluation in replication and pathogenesis in animal models. These results suggest that nsp 4 has dispensable regions for replication, or that it possibly has domains that are dedicated to other functions not directly related to virus replication.

3.4. Nsp 14

Nsp 14 is an ORF1b protein that is downstream from nsp 12 (RdRp) and nsp 13 (helicase/NTPase/RNA 5′-triphosphatase) and upstream from nsp 15 (nidovirus uridylate-specific

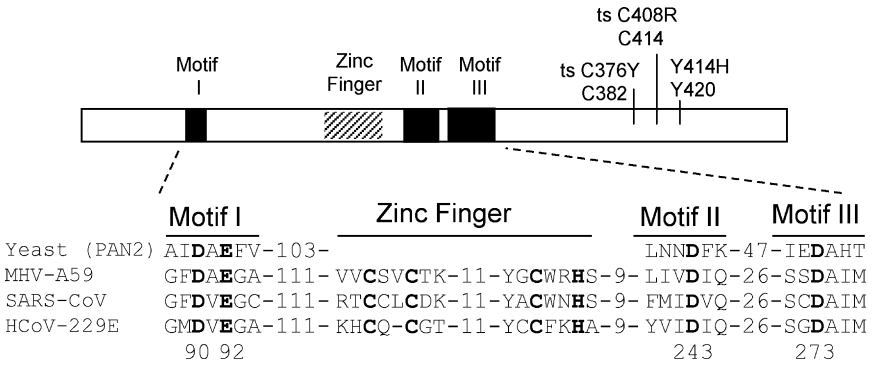

Fig. 6. Motifs and substitution sites in nsp 14. The organization of nsp 14 is shown. Exonuclease motifs I through III (black boxes) and a putative zinc finger motif (hatched box) are shown. Location of reported MHV mutations conferring a ts phenotype are shown by residue number and substitution, along with the conserved SARS-CoV residues below. The virulence-attenuating Y414H mutant of MHV is shown, with conserved SARS-CoV Y420. A partial sequence alignment of coronavirus nsp 14 sequences from MHV-A59, SARS-CoV, and human coronavirus 229E with that of *S. cerevisiae* PAN2, a poly(A)-specific exoribonuclease, is shown at the bottom. Completely conserved exonuclease active site and zinc-coordinating residues are shown in bold, with DE-D-D aa numbers shown for SARS-CoV.

endoribonuclease) and nsp 16 (putative 2′-*O*-RNA methyltransferase) (Bhardwaj et al., 2004; Ivanov et al., 2004a,b; Snijder et al., 2003; Thiel et al., 2003). The expression of nsp 14, which is cleaved from nsps 13 and 15 by nsp 5, is proposed to involve an intermediate precursor of nsps 12–16 (Denison et al., 1991). Nsp 14 likely functions coordinately with nsps 15 and 16 in processing and modification of viral or cellular RNAs. Nsp 14 was first predicted, and more recently demonstrated in biochemical studies using bacterially expressed and purified full-length nsp 14, to possess 3′–5′ exonuclease activity on RNA but not on DNA substrates (Minskaia et al., 2006; Snijder et al., 2003). All coronavirus nsp 14 sequences have conserved putative active site residues that allow assignment of nsp 14 to the DE-D-D superfamily of exonucleases, named after the four invariant acidic residues of the active site (Fig. 6). Alanine substitution of the conserved active site residues diminished or eliminated exonuclease activity of purified SARS-CoV nsp 14 in vitro. When alanine substitution of the active site DE or other residues was engineered in the context of the full-length infectious clone of HCoV-229E, genomic and subgenomic viral RNAs were detected in transfected cells but no virus was recovered, suggesting that nsp 14 was essential for virus replication (Minskaia et al., 2006).

The initial studies of MHV nsp 14 resulted from the observation that the original recombinant clone of MHV-A59 was phenotypically wildtype in all aspects of growth in cell culture, but surprisingly had no measurable LD_{50} and appeared completely attenuated in mice (Sperry et al., 2005). This unexpected result led to comprehensive sequencing of the cloned cDNA fragments used to assemble the full-length MHV cDNA, and analysis identified two single-nucleotide mutations, each resulting in nonconservative amino acid substitutions: one at Y414 in nsp 14 and one in an accessory protein unique to MHV, the ORF2a protein. Sequencing of recombinant virus confirmed the presence of the Y414H substitution. When the wildtype Y414 and mutant Y414H cDNAs were compared, both displayed wildtype growth in cell culture. However, the Y414 virus was virulent in mice, whereas the Y414H mutant was completely attenuated, even in the absence of the mutation in the 2a protein (Sperry et al., 2005). This was the first demonstration in coronavirus ORF1ab of a mutation that does not impact replication in culture but attenuates virulence in an animal host, and thus, this study provides strong evidence for a role of nsp 14 distinct from or in addition to any function in replication.

The above results led to a reconsideration of the domain organization of nsp 14 and possible functions in replication and pathogenesis. The exoribonuclease (ExoN) motifs of nsp 14 are located in the amino-terminal half of the 521-aa MHV nsp 14 protein (SARS-CoV nsp 14 is 527 aa). In contrast, the Y414 residue is in the carboxy-terminal half of the protein, which has no predicted role in ExoN activity, no known function, and no significant homology to other proteins. To address the role of nsp 14 in MHV replication, a variety of mutations and deletions, including deletion of the proteinase cleavage sites at either terminus of nsp14, substitution of ExoN catalytic residues, substitution of Y414 with other amino acids, and deletion of Y414 (Fig. 6) (Eckerle et al., 2006) was engineered in the nsp14 coding sequence and tested for virus viability and growth in cell culture. When P1-Gln of either the nsp 13 | nsp 14 or the nsp 14 | nsp 15 cleavage site was deleted, mutant viruses were recovered, although the growth of the nsp 13 | nsp 14 cleavage site mutant is markedly delayed. Most nsp 14 Y414 substitution mutants were recovered and demonstrated near or equivalent to wildtype growth in culture. When the Y414H substitution was recapitulated at the conserved SARS-CoV Y420 residue, viable virus was recovered and is currently being analyzed for its effect on SARS-CoV replication and virulence in animal models.

The results of the current and previous studies on nsp 14 raise important questions concerning the role of nsp 14 in RNA processing, virus replication, and pathogenesis. Are the natural substrates of ExoN activity viral or cellular RNAs? Does the carboxy-terminal half of nsp 14 modulate ExoN activity, and if so, is Y414 involved? Does nsp 14 serve other functions in virus replication? Does the protein have a unique role in subgenomic RNA synthesis? Is ExoN activity required for coronavirus replication and virulence in animals? What is the mechanism of attenuation caused by the Y414H substitution in MHV nsp 14? To answer these questions, it will be essential to develop

biochemical assays with nsp 14 from other coronaviruses and to determine the effects of additional nsp 14 mutations in both MHV and SARS-CoV on virus replication, viral RNA synthesis, and virulence.

3.5. Other nsps: structures and mutants lead the way

Most coronaviruses express and process 15 or 16 confirmed or predicted mature proteins from their OR1ab polyproteins, in addition to at least three intermediate precursors that may have additional functions. It is beyond the scope of this review to detail the putative functions, cell biology, and mutagenesis of all of these proteins. However, in relation to viral pathogenesis, important strides have been made in providing a basis for studies of these proteins in the pathogenesis of SARS-CoV and other coronaviruses. First, the structures have been reported for all or parts of nsp 3, 5 (3CLpro or Mpro), 7–10, and 15 (Bhardwaj et al., 2006; Chou et al., 2004; Egloff et al., 2004; Joseph et al., 2006; Lee et al., 2005; Ratia et al., 2006; Ricagno et al., 2006; Saikatendu et al., 2005; Su et al., 2006; Sutton et al., 2004; Tan et al., 2005; Zhai et al., 2005). These results show remarkable multimeric protein interactions, raising important questions about the expression and interactions of the proteins as they are processed from the ORF1ab polyprotein. For example, how does the proposed hexameric structure of nsp 15 (Xu et al., 2006) interact with the proposed dodecameric structure of nsp 10 (Joseph et al., 2006; Su et al., 2006)?

Second, a recent careful analysis of long established temperature-sensitive MHV mutants has defined new targets for the rich interface between forward and reverse genetic analyses of SARS-CoV and other coronaviruses in replication and pathogenesis. Sawicki et al. performed sequencing of ORF1 from a large panel of available temperature-sensitive (ts) mutants with different conditional defects, including lethality, that were generated in several labs and were the basis for establishing complementation groups (Sawicki et al., 2005). The report identified single point mutations resulting in nonsynonymous substitutions in nsps 4, 5, 10, 12, 14 and 16. The overall results suggest that the ORF1b nsp 12, 14 and 16 proteins define distinct cistrons, while the mutants in ORF1a proteins nsps 4, 5, and 10 form a single complementation group, a conclusion that is in line with the proposed processing schemes and location in the ORF1ab coding sequence. Additionally, the study provides some valuable insights. Notably, of the eight reported ts mutations in MHV, seven of the affected amino acid residues are identical in SARS-CoV, and the eighth was Asn in MHV nsp 4 and Asp in SARS-CoV nsp 4. While the mutants were analyzed for their conditional growth defects and possible roles in RNA synthesis, it should be possible to reproduce the amino acid changes using multiple nucleotide mutations, thus stabilizing the amino acid substitution. This approach may allow selection of phenotypic revertants that will identify protein interactions and new functions in both replication and pathogenesis. In addition, it will allow the changes to be introduced in SARS-CoV to determine if the ts phenotype can be recreated in that background, with the possibility of rapidly establishing a panel of SARS-CoV conditional growth mutants.

4. Conclusions

The exciting advances in the evolution, genetics, replication and pathogenesis of SARS-CoV and other coronaviruses has raised many important questions concerning the role of ORF1ab proteins in all of the stages that comprise the pathogenic pathway of SARS-CoV:

1. Do the changes across the replicase from bats to civets to humans represent important host range or pathogenic determinants? Do the patterns of change reflect host-specific adaptations in replication or virulence?
2. Are SARS-CoV mutants within ORF1ab proteins or processing networks from other coronaviruses viable, and if so, are they altered in replication and virulence in animal models?
3. Are replicase proteins specifically altering host gene expression, and specifically pathways that alter immune response?
4. Do mutations and deletions in SARS-CoV nsp 1 alter interferon and cytokine responses in infected cells or animals?
5. Are replicase proteins altering host gene expression or immune response in ways that are virus- and/or host-specific?
6. Can avirulent SARS-CoV replicase mutants provide protective immunity from wildtype SARS-CoV infection?

Addressing these questions will help us further our understanding of the interplay between SARS-CoV replication and pathogenesis in the host.

Acknowledgments

The authors gratefully acknowledge the technical assistance of XiaoTao Lu and Steven Sperry. This work was supported by National Institutes of Health grants RO1 AI26603, AI50083, and PO1AI059443-01.

References

Anand, K., Ziebuhr, J., Wadhwani, P., Mesters, J.R., Hilgenfeld, R., 2003. Coronavirus main proteinase (3CLpro) structure: basis for design of anti-SARS drugs. Science 300 (5626), 1763–1767.

Baranov, P.V., Henderson, C.M., Anderson, C.B., Gesteland, R.F., Atkins, J.F., Howard, M.T., 2005. Programmed ribosomal frameshifting in decoding the SARS-CoV genome. Virology 332 (2), 498–510.

Baric, R.S., Yount, B., Hensley, L., Peel, S.A., Chen, W., 1997. Episodic evolution mediates interspecies transfer of a murine coronavirus. J. Virol. 71 (3), 1946–1955.

Barretto, N., Jukneliene, D., Ratia, K., Chen, Z., Mesecar, A.D., Baker, S.C., 2005. The papain-like protease of severe acute respiratory syndrome coronavirus has deubiquitinating activity. J. Virol. 79 (24), 15189–15198.

Bhardwaj, K., Guarino, L., Kao, C.C., 2004. The severe acute respiratory syndrome coronavirus Nsp15 protein is an endoribonuclease that prefers manganese as a cofactor. J. Virol. 78 (22), 12218–12224.

Bhardwaj, K., Sun, J., Holzenburg, A., Guarino, L.A., Kao, C.C., 2006. RNA recognition and cleavage by the SARS coronavirus endoribonuclease. J. Mol. Biol. 361 (2), 243–256.

Bonilla, P.J., Gorbalenya, A.E., Weiss, S.R., 1994. Mouse hepatitis virus strain A59 RNA polymerase gene ORF 1a: heterogeneity among MHV strains. Virology 198 (2), 736–740.

Bonilla, P.J., Hughes, S.A., Pinon, J.D., Weiss, S.R., 1995. Characterization of the leader papain-like proteinase of MHV-A59: identification of a new in vitro cleavage site. Virology 209 (2), 489–497.

Bonilla, P.J., Hughes, S.A., Weiss, S.R., 1997. Characterization of a second cleavage site and demonstration of activity in trans by the papain-like proteinase of the murine coronavirus mouse hepatitis virus strain A59. J. Virol. 71 (2), 900–909.

Bost, A.G., Carnahan, R.H., Lu, X.T., Denison, M.R., 2000. Four proteins processed from the replicase gene polyprotein of mouse hepatitis virus colocalize in the cell periphery and adjacent to sites of virion assembly. J. Virol. 74 (7), 3379–3387.

Bost, A.G., Prentice, E., Denison, M.R., 2001. Mouse hepatitis virus replicase protein complexes are translocated to sites of M protein accumulation in the ERGIC at late times of infection. Virology 285, 21–29.

Brockway, S.M., Denison, M.R., 2005. Mutagenesis of the murine hepatitis virus nsp1-coding region identifies residues important for protein processing, viral RNA synthesis, and viral replication. Virology 340 (2), 209–223.

Brockway, S.M., Lu, X.T., Peters, T.R., Dermody, T.S., Denison, M.R., 2004. Intracellular localization and protein interactions of the gene 1 protein p28 during mouse hepatitis virus replication. J. Virol. 78 (21), 11551–11562.

Chinese, S.M.E.C., 2004. Molecular evolution of the SARS coronavirus during the course of the SARS epidemic in China. Science 303 (5664), 1666–1669.

Chou, C.Y., Chang, H.C., Hsu, W.C., Lin, T.Z., Lin, C.H., Chang, G.G., 2004. Quaternary structure of the severe acute respiratory syndrome (SARS) coronavirus main protease. Biochemistry 43 (47), 14958–14970.

Darnell, M.E., Subbarao, K., Feinstone, S.M., Taylor, D.R., 2004. Inactivation of the coronavirus that induces severe acute respiratory syndrome, SARS-CoV. J. Virol. Meth. 121 (1), 85–91.

Denison, M.R., Sims, A.C., Gibson, C.A., Lu, X.T., 1998. Processing of the MHV-A59 gene 1 polyprotein by the 3C-like proteinase. Adv. Exp. Med. Biol. 440, 121–127.

Denison, M.R., Spaan, W.J., van der Meer, Y., Gibson, C.A., Sims, A.C., Prentice, E., Lu, X.T., 1999. The putative helicase of the coronavirus mouse hepatitis virus is processed from the replicase gene polyprotein and localizes in complexes that are active in viral RNA synthesis. J. Virol. 73 (8), 6862–6871.

Denison, M.R., Yount, B., Brockway, S.M., Graham, R.L., Sims, A.C., Lu, X., Baric, R.S., 2004. Cleavage between replicase proteins p28 and p65 of mouse hepatitis virus is not required for virus replication. J. Virol. 78 (11), 5957–5965.

Denison, M.R., Zoltick, P.W., Hughes, S.A., Giangreco, B., Olson, A.L., Perlman, S., Leibowitz, J.L., Weiss, S.R., 1992. Intracellular processing of the N-terminal ORF 1a proteins of the coronavirus MHV-A59 requires multiple proteolytic events. Virology 189 (1), 274–284.

Denison, M.R., Zoltick, P.W., Leibowitz, J.L., Pachuk, C.J., Weiss, S.R., 1991. Identification of polypeptides encoded in open reading frame 1b of the putative polymerase gene of the murine coronavirus mouse hepatitis virus A59. J. Virol. 65 (6), 3076–3082.

Dong, S., Baker, S.C., 1994. Determinants of the p28 cleavage site recognized by the first papain-like cysteine proteinase of murine coronavirus. Virology 204 (2), 541–549.

Dos Ramos, F., Carrasco, M., Doyle, T., Brierley, I., 2004. Programmed-1 ribosomal frameshifting in the SARS coronavirus. Biochem. Soc. Trans. 32 (Pt 6), 1081–1083.

Eckerle, L.D., Brockway, S.M., Sperry, S.M., Lu, X., Denison, M.R., 2006. Effects of mutagenesis of murine hepatitis virus nsp1 and nsp14 on replication in culture. Adv. Exp. Med. Biol. 581, 55–60.

Egloff, M.P., Ferron, F., Campanacci, V., Longhi, S., Rancurel, C., Dutartre, H., Snijder, E.J., Gorbalenya, A.E., Cambillau, C., Canard, B., 2004. The severe acute respiratory syndrome-coronavirus replicative protein nsp9 is a single-stranded RNA-binding subunit unique in the RNA virus world. Proc. Natl. Acad. Sci. USA 101 (11), 3792–3796.

Fischer, F., Stegen, C., Masters, P., Samsonoff, W., 1998. Analysis of constructed E gene mutants of mouse hepatitis virus confirms a pivotal role for E protein in coronavirus assembly. J. Virol. 72 (10), 7885–7894.

Gao, H.Q., Schiller, J.J., Baker, S.C., 1996. Identification of the polymerase polyprotein products p72 and p65 of the murine coronavirus MHV-JHM. Virus Res. 45 (2), 101–109.

Gosert, R., Kanjanahaluethai, A., Egger, D., Bienz, K., Baker, S.C., 2002. RNA replication of mouse hepatitis virus takes place at double-membrane vesicles. J. Virol. 76 (8), 3697–3708.

Graham, R.L., Denison, M.R., 2006. Replication of murine hepatitis virus is regulated by papain-like proteinase 1 processing of nonstructural proteins 1, 2, and 3. J. Virol. 80, 11610–11620.

Graham, R.L., Sims, A.C., Baric, R.S., Denison, M.R., 2006. The nsp2 proteins of mouse hepatitis virus and SARS coronavirus are dispensable for viral replication. Adv. Exp. Med. Biol. 581, 67–72.

Graham, R.L., Sims, A.C., Brockway, S.M., Baric, R.S., Denison, M.R., 2005. The nsp2 replicase proteins of murine hepatitis virus and severe acute respiratory syndrome coronavirus are dispensable for viral replication. J. Virol. 79 (21), 13399–13411.

Han, Y.S., Chang, G.G., Juo, C.G., Lee, H.J., Yeh, S.H., Hsu, J.T., Chen, X., 2005. Papain-like protease 2 (PLP2) from severe acute respiratory syndrome coronavirus (SARS-CoV): expression, purification, characterization, and inhibition. Biochemistry 44 (30), 10349–10359.

Harcourt, B.H., Jukneliene, D., Kanjanahaluethai, A., Bechill, J., Severson, K.M., Smith, C.M., Rota, P.A., Baker, S.C., 2004. Identification of severe acute respiratory syndrome coronavirus replicase products and characterization of papain-like protease activity. J. Virol. 78 (24), 13600–13612.

Huang, I.C., Bosch, B.J., Li, W., Farzan, M., Rottier, P.M., Choe, H., 2006. SARS-CoV, but not HCoV-NL63, utilizes cathepsins to infect cells: viral entry. Adv. Exp. Med. Biol. 581, 335–338.

Ivanov, K.A., Hertzig, T., Rozanov, M., Bayer, S., Thiel, V., Gorbalenya, A.E., Ziebuhr, J., 2004a. Major genetic marker of nidoviruses encodes a replicative endoribonuclease. Proc. Natl. Acad. Sci. USA 101 (34), 12694–12699.

Ivanov, K.A., Thiel, V., Dobbe, J.C., van der Meer, Y., Snijder, E.J., Ziebuhr, J., 2004b. Multiple enzymatic activities associated with severe acute respiratory syndrome coronavirus helicase. J. Virol. 78 (11), 5619–5632.

Joseph, J.S., Saikatendu, K.S., Subramanian, V., Neuman, B.W., Brooun, A., Griffith, M., Moy, K., Yadav, M.K., Velasquez, J., Buchmeier, M.J., Stevens, R.C., Kuhn, P., 2006. Crystal structure of nonstructural protein 10 from the severe acute respiratory syndrome coronavirus reveals a novel fold with two zinc-binding motifs. J. Virol. 80 (16), 7894–7901.

Kamitani, W., Narayanan, K., Huang, C., Lokugamage, K., Ikegami, T., Ito, N., Kubo, H., Makino, S., 2006. Severe acute respiratory syndrome coronavirus nsp1 protein suppresses host gene expression by promoting host mRNA degradation. Proc. Natl. Acad. Sci. USA 103 (34), 12885–12890.

Kanjanahaluethai, A., Baker, S.C., 2001. Processing of the replicase of murine coronavirus: papain-like proteinase 2 (PLP2) acts to generate p150 and p44. Adv. Exp. Med. Biol. 494, 267–273.

Kanjanahaluethai, A., Jukneliene, D., Baker, S.C., 2003. Identification of the murine coronavirus MP1 cleavage site recognized by papain-like proteinase 2. J. Virol. 77 (13), 7376–7382.

Klumperman, J., Krijnse Locker, J., Meijer, A., Horzinek, M.C., Geuze, H.J., Rottier, P.J.M., 1994. Coronavirus M protein accumulates in the Golgi complex beyond the site of virion budding. J. Virol. 68 (10), 6523–6534.

Krijnse-Locker, J., Ericsson, M., Rottier, P.J., Griffiths, G., 1994. Characterization of the budding compartment of mouse hepatitis virus: evidence that transport from the RER to the Golgi complex requires only one vesicular transport step. J. Cell Biol. 124 (1–2), 55–70.

Law, A.H., Lee, D.C., Cheung, B.K., Yim, H.C., Lau, A.S., 2006. A role for the non-structural protein-1 of SARS-coronavirus in chemokine dysregulation. J. Virol. 81, 416–422.

Lee, T.W., Cherney, M.M., Huitema, C., Liu, J., James, K.E., Powers, J.C., Eltis, L.D., James, M.N., 2005. Crystal structures of the main peptidase from the SARS coronavirus inhibited by a substrate-like aza-peptide epoxide. J. Mol. Biol. 353 (5), 1137–1151.

Li, W., Moore, M.J., Vasilieva, N., Sui, J., Wong, S.K., Berne, M.A., Somasundaran, M., Sullivan, J.L., Luzuriaga, K., Greenough, T.C., Choe, H., Farzan, M., 2003. Angiotensin-converting enzyme 2 is a functional receptor for the SARS coronavirus. Nature 426 (6965), 450–454.

Lindner, H.A., Fotouhi-Ardakani, N., Lytvyn, V., Lachance, P., Sulea, T., Menard, R., 2005. The papain-like protease from the severe acute respiratory syndrome coronavirus is a deubiquitinating enzyme. J. Virol. 79 (24), 15199–15208.

Lu, X.T., Lu, Y.Q., Denison, M.R., 1996. Intracellular and in vitro translated 27-kDa proteins contain the 3C-like proteinase activity of the coronavirus MHV-A59. Virology 222, 375–382.

Lu, X.T., Sims, A.C., Denison, M.R., 1998. Mouse hepatitis virus 3C-like protease cleaves a 22-kilodalton protein from the open reading frame 1a polyprotein in virus-infected cells and in vitro. J. Virol. 72 (3), 2265–2271.

Minskaia, E., Hertzig, T., Gorbalenya, A.E., Campanacci, V., Cambillau, C., Canard, B., Ziebuhr, J., 2006. Discovery of an RNA virus 3′→5′ exoribonuclease that is critically involved in coronavirus RNA synthesis. Proc. Natl. Acad. Sci. USA 103 (13), 5108–5113.

Narayanan, K., Maeda, A., Maeda, J., Makino, S., 2000. Characterization of the coronavirus M protein and nucleocapsid interaction in infected cells. J. Virol. 74 (17), 8127–8134.

Opstelten, D., Horzinek, M., Rottier, P., 1993. Complex formation between the spike protein and the membrane protein during mouse hepatitis virus assembly. Adv. Exp. Med. Biol. 342, 189.

Opstelten, D.J., Raamsman, M.J., Wolfs, K., Horzinek, M.C., Rottier, P.J., 1995. Envelope glycoprotein interactions in coronavirus assembly. J. Cell Biol. 131 (2), 339–349.

Prentice, E., Jerome, W.G., Yoshimori, T., Mizushima, N., Denison, M.R., 2004a. Coronavirus replication complex formation utilizes components of cellular autophagy. J. Biol. Chem. 279 (11), 10136–10141.

Prentice, E., McAuliffe, J., Lu, X., Subbarao, K., Denison, M.R., 2004b. Identification and characterization of severe acute respiratory syndrome coronavirus replicase proteins. J. Virol. 78 (18), 9977–9986.

Putics, A., Filipowicz, W., Hall, J., Gorbalenya, A.E., Ziebuhr, J., 2005. ADP-ribose-1″-monophosphatase: a conserved coronavirus enzyme that is dispensable for viral replication in tissue culture. J. Virol. 79 (20), 12721–12731.

Raamsman, M.J., Krijnse Locker, J., de Hooge, A., de Vries, A.F., Griffiths, G., Vennema, H., Rottier, P.J., 2000. Characterization of the coronavirus mouse hepatitis strain A59 small membrane protein E. J. Virol. 74 (5), 2333–2342.

Ratia, K., Saikatendu, K.S., Santarsiero, B.D., Barretto, N., Baker, S.C., Stevens, R.C., Mesecar, A.D., 2006. Severe acute respiratory syndrome coronavirus papain-like protease: structure of a viral deubiquitinating enzyme. Proc. Natl. Acad. Sci. USA 103 (15), 5717–5722.

Ricagno, S., Egloff, M.P., Ulferts, R., Coutard, B., Nurizzo, D., Campanacci, V., Cambillau, C., Ziebuhr, J., Canard, B., 2006. Crystal structure and mechanistic determinants of SARS coronavirus nonstructural protein 15 define an endoribonuclease family. Proc. Natl. Acad. Sci. USA 103 (32), 11892–11897.

Roberts, A., Deming, D., Paddock, C.D., Cheng, A., Yount, B., Vogel, L., Herman, B.D., Sheahan, T., Heise, M., Genrich, G.L., Zaki, S.R., Baric, R., Subbarao, K., 2007. A mouse-adapted SARS-coronavirus causes disease and mortality in BALB/c mice. PLoS Pathog. 3, 23–37.

Saikatendu, K.S., Joseph, J.S., Subramanian, V., Clayton, T., Griffith, M., Moy, K., Velasquez, J., Neuman, B.W., Buchmeier, M.J., Stevens, R.C., Kuhn, P., 2005. Structural basis of severe acute respiratory syndrome coronavirus ADP-ribose-1″-phosphate dephosphorylation by a conserved domain of nsP3. Structure (Camb.) 13 (11), 1665–1675.

Sawicki, S.G., Sawicki, D.L., 2005. Coronavirus transcription: a perspective. Curr. Top Microbiol. Immunol. 287, 31–55.

Sawicki, S.G., Sawicki, D.L., Siddell, S.G., 2007. A contemporary view of coronavirus transcription. J. Virol. 81 (1), 20–29.

Sawicki, S.G., Sawicki, D.L., Younker, D., Meyer, Y., Thiel, V., Stokes, H., Siddell, S.G., 2005. Functional and genetic analysis of coronavirus replicase-transcriptase proteins. PLoS Pathog. 1 (4), e39.

Schiller, J.J., Kanjanahaluethai, A., Baker, S.C., 1998. Processing of the coronavirus mhv-jhm polymerase polyprotein: identification of precursors and proteolytic products spanning 400 kilodaltons of ORF1a. Virology 242, 288–302.

Simmons, G., Gosalia, D.N., Rennekamp, A.J., Reeves, J.D., Diamond, S.L., Bates, P., 2005. Inhibitors of cathepsin L prevent severe acute respiratory syndrome coronavirus entry. Proc. Natl. Acad. Sci. USA 102 (33), 11876–11881.

Sims, A.C., Ostermann, J., Denison, M.R., 2000. Mouse hepatitis virus replicase proteins associate with two distinct populations of intracellular membranes. J. Virol. 74 (12), 5647–5654.

Snijder, E.J., Bredenbeek, P.J., Dobbe, J.C., Thiel, V., Ziebuhr, J., Poon, L.L., Guan, Y., Rozanov, M., Spaan, W.J., Gorbalenya, A.E., 2003. Unique and conserved features of genome and proteome of SARS-coronavirus, an early split-off from the coronavirus group 2 lineage. J. Mol. Biol. 331 (5), 991–1004.

Sperry, S.M., Kazi, L., Graham, R.L., Baric, R.S., Weiss, S.R., Denison, M.R., 2005. Single-amino-acid substitutions in open reading frame (ORF) 1b-nsp14 and ORF 2a proteins of the coronavirus mouse hepatitis virus are attenuating in mice. J. Virol. 79 (6), 3391–3400.

Su, D., Lou, Z., Sun, F., Zhai, Y., Yang, H., Zhang, R., Joachimiak, A., Zhang, X.C., Bartlam, M., Rao, Z., 2006. Dodecamer structure of severe acute respiratory syndrome coronavirus nonstructural protein nsp10. J. Virol. 80 (16), 7902–7908.

Sutton, G., Fry, E., Carter, L., Sainsbury, S., Walter, T., Nettleship, J., Berrow, N., Owens, R., Gilbert, R., Davidson, A., Siddell, S., Poon, L.L., Diprose, J., Alderton, D., Walsh, M., Grimes, J.M., Stuart, D.I., 2004. The nsp9 replicase protein of SARS-coronavirus, structure and functional insights. Structure 12 (2), 341–353.

Tan, J., Verschueren, K.H., Anand, K., Shen, J., Yang, M., Xu, Y., Rao, Z., Bigalke, J., Heisen, B., Mesters, J.R., Chen, K., Shen, X., Jiang, H., Hilgenfeld, R., 2005. pH-dependent conformational flexibility of the SARS-CoV main proteinase (M(pro)) dimer: molecular dynamics simulations and multiple X-ray structure analyses. J. Mol. Biol. 354 (1), 25–40.

Teng, H., Pinon, J.D., Weiss, S.R., 1999. Expression of murine coronavirus recombinant papain-like proteinase: efficient cleavage is dependent on the lengths of both the substrate and the proteinase polypeptides. J. Virol. 73 (4), 2658–2666.

Thiel, V., Ivanov, K.A., Putics, A., Hertzig, T., Schelle, B., Bayer, S., Weissbrich, B., Snijder, E.J., Rabenau, H., Doerr, H.W., Gorbalenya, A.E., Ziebuhr, J., 2003. Mechanisms and enzymes involved in SARS coronavirus genome expression. J. Gen. Virol. 84 (Pt 9), 2305–2315.

van der Meer, Y., Snijder, E.J., Dobbe, J.C., Schleich, S., Denison, M.R., Spaan, W.J., Locker, J.K., 1999. Localization of mouse hepatitis virus nonstructural proteins and RNA synthesis indicates a role for late endosomes in viral replication. J. Virol. 73 (9), 7641–7657.

Xu, X., Zhai, Y., Sun, F., Lou, Z., Su, D., Xu, Y., Zhang, R., Joachimiak, A., Zhang, X.C., Bartlam, M., Rao, Z., 2006. New antiviral target revealed by the hexameric structure of mouse hepatitis virus nonstructural protein nsp15. J. Virol. 80 (16), 7909–7917.

Yount, B., Curtis, K.M., Fritz, E.A., Hensley, L.E., Jahrling, P.B., Prentice, E., Denison, M.R., Geisbert, T.W., Baric, R.S., 2003. Reverse genetics with a full-length infectious cDNA of severe acute respiratory syndrome coronavirus. Proc. Natl. Acad. Sci. USA 100 (22), 12995–13000.

Yount, B., Denison, M.R., Weiss, S.R., Baric, R.S., 2002. Systematic assembly of a full-length infectious cDNA of mouse hepatitis virus strain A59. J. Virol. 76 (21), 11065–11078.

Yount, B., Roberts, R.S., Sims, A.C., Deming, D., Frieman, M.B., Sparks, J., Denison, M.R., Davis, N., Baric, R.S., 2005. Severe acute respiratory syndrome coronavirus group-specific open reading frames encode nonessential functions for replication in cell cultures and mice. J. Virol. 79 (23), 14909–14922.

Zhai, Y., Sun, F., Li, X., Pang, H., Xu, X., Bartlam, M., Rao, Z., 2005. Insights into SARS-CoV transcription and replication from the structure of the nsp7–nsp8 hexadecamer. Nat. Struct. Mol. Biol. 12 (11), 980–986.

Ziebuhr, J., Snijder, E.J., Gorbalenya, A.E., 2000. Virus-encoded proteinases and proteolytic processing in the Nidovirales. J. Gen. Virol. 81 (Pt 4), 853–879.